ELSEVIER

Journal of Fluids and Structures 19 (2004) 943–956

JOURNAL OF FLUIDS AND STRUCTURES

www.elsevier.nl/locate/jnlabr/yjfls

Fluidelastic instability of flexible tubes subjected to two-phase internal flow

C. Monette, M.J. Pettigrew*

Mechanical Engineering Department, École Polytechnique, P.O. Box 6079, Station Centre-Ville, Montréal, Que., Canada, H3C 3A7

Received 6 June 2004; accepted 11 June 2004

Abstract

The fluidelastic instability behaviour of flexible tubes subjected to internal single-phase (liquid or gas) flows is now reasonably well understood. Although many piping systems operate in two-phase flows, so far very little work has been done to study their dynamic behaviour under such flows. This paper presents the results of a series of experiments to study the fluidelastic instability behaviour of flexible tubes subjected to two-phase internal flow. Several flexible tubes of different diameters, lengths and flexural rigidities were tested over a broad range of flow velocities and void fractions in an air–water loop to simulate two-phase flows. Well-defined fluidelastic instabilities were observed in two-phase flows. The existing theory to formulate the fluidelastic behaviour under internal flow was developed further to take into account two-phase flow. The agreement between the experimental results and the modified theory is remarkably good. However, it depends on using an appropriate model to formulate the characteristics of the two-phase flows.

1. Introduction

The fluidelastic instability behaviour of flexible tubes subjected to internal single-phase (liquid or gas) flow is now reasonably well understood as outlined by Paidoussis (1998). Although many piping systems operate in two-phase flows, so far very little work has been done to study their dynamic behaviour under such flows. The fluidelastic behaviour of flexible cylinders subjected to two-phase annular axial flows was investigated in the mid-1970s for the development of nuclear fuels for boiling water reactors (BWR) (Pettigrew and Paidoussis, 1975; Païdoussis and Pettigrew, 1979). Although well-defined fluidelastic instabilities were observed in single-phase annular flow, instabilities under two-phase conditions remained elusive in spite of much effort to observe them. This somewhat unexpected behaviour led to a variety of explanations such as the existence of nonlinearities due to the proximity of the annular flow boundary, the excessive turbulence of air–water mixtures inhibiting the initiation of instability, and the relatively larger damping associated with two-phase flows. Thus, to the knowledge of the authors, the possibility of fluidelastic instability in axial two-phase flows has not yet been established.

A number of studies were undertaken in the 1980s and early 1990s (Pettigrew et al., 1989; Pettigrew and Taylor, 1994; Axisa et al., 1985; Nakamura et al., 1995) to investigate the vibration behaviour of tube bundles in two-phase cross-flow. This work was largely related to nuclear steam generators. Fluidelastic instabilities were generally observed for

*Corresponding author.
E-mail address: michel.pettigrew@polymtl.ca (M.J. Pettigrew).

0889-9746/$ - see front matter
doi:10.1016/j.jfluidstructs.2004.06.003

Nomenclature

A	tube internal cross-sectional area
A_g	area occupied by the gas in the tube internal cross-section
A_l	area occupied by the liquid in the tube internal cross-section
EI	tube flexural rigidity
F	frequency (Hz)
g	gravitational acceleration
K	slip ratio defined by $K = U_g/U_l$
k	viscous damping coefficient
L	length of tube
M	mass of fluid per unit length
m	mass of tube per unit length
p	tube internal pressure
Q_g	volumetric gas flow rate
Q_l	volumetric liquid flow rate
T	axial tension in tube
t	time
U	average flow velocity
$U_{g,a}$	average gas (or air) velocity
$U_{l,w}$	average liquid (or water) velocity
u	dimensionless flow velocity defined by $u = (M/EI)^{1/2}UL$
u_c	dimensionless critical flow velocity
u_w	dimensionless critical water velocity defined by $u_w = (M_w/EI)^{1/2}U_wL$
u_a	dimensionless critical air velocity defined by $u_a = (M_a/EI)^{1/2}U_aL$
x	longitudinal coordinate
y	lateral deflection of the tube
α	void fraction
β	dimensionless mass ratio $M/(M+m)$
γ	dimensionless parameter defined by the tube length and the gravitational acceleration $\gamma = (M+m)gL^3/EI$
ε_g	volumetric quality
η	dimensionless lateral deflection of the tube defined by $\eta = y/L$
κ	dimensionless viscous damping coefficient defined by $\kappa = [(M+m)/EI]^{1/2}k/L$
λ_r	eigenvalues of cantilever for mode r
μ	hysteretic structural damping coefficient
ξ	dimensionless longitudinal coordinate defined by $\xi = x/L$
ρ_g	gas volumetric mass
ρ_l	liquid volumetric mass
ρ_H	homogeneous volumetric mass
τ	dimensionless time defined by $\tau = \{EI/[(M+m)]L^4\}^{1/2}t$
ϕ_r	eigenfunctions of cantilever for mode r
Ω	circular frequency (rad/s)
ω	dimensionless frequency defined by $\omega = [(M+m/EI)]^{1/2}\Omega L^2$
ω_c	dimensionless critical frequency

Other symbols are defined in the text.

straight tube bundles in air–water cross-flow. Particularly well-defined instabilities were seen in the much less turbulent two-phase Freon cross-flows (Pettigrew et al., 1994, 2002; Feenstra et al., 1995, 2002). On the other hand, well-defined instabilities were only observed in liquid and in very low void fraction air–water cross-flows for U-tube bundles (Boucher and Taylor, 1996). Why instabilities were not observed at the higher void fractions may be explained by the overwhelming response to turbulence or by nonlinear effects due to the closeness of neighbouring tubes in the relatively more flexible U-tube bundle. Thus, a better understanding of fluidelastic instability in two-phase flows is generally required. Hopefully, this paper is a step in that direction from the point of view of axial flow.

This paper presents the results of a series of experiments to study the fluidelastic instability behaviour of cantilevered flexible tubes subjected to two-phase internal flow. Several flexible tubes of different diameters, lengths and flexural rigidities were tested over a broad range of flow velocities and void fractions in an air–water loop to simulate two-phase flows. Well-defined fluidelastic instabilities were observed.

The existing theory to formulate the fluidelastic behaviour under internal flow was developed further to take into account two-phase flow. Several models are available to formulate the characteristics of two-phase flows. Although these models were developed from a thermal-hydraulics point of view, they were evaluated from the perspective of their appropriateness to represent the fluidelastic instability parameters. A modified two-phase model emerged that provided remarkably good agreement between the experimental results and the modified theory.

The experimental results, the development of the modified theory, the evaluation of the two-phase flow models and a comparison between experimental results and theory are presented in this paper.

2. Fluidelastic instability theory

2.1. Single-phase flow

Paidoussis (1970,1998) has developed the force equilibrium equations to formulate fluidelastic instability for cantilever tubes subjected to internal flows:

$$EI\frac{\partial^4 y}{\partial x^4}+(M+m)g\left((x-L)\frac{\partial^2 y}{\partial x^2}+\frac{\partial y}{\partial x}\right)+MU^2\frac{\partial^2 y}{\partial x^2}+2MU\frac{\partial^2 y}{\partial t\partial x}+(M+m)\frac{\partial^2 y}{\partial t^2}+EI\frac{\mu}{\Omega}\frac{\partial}{\partial t}\left(\frac{\partial^4 y}{\partial x^4}\right)+k\frac{\partial y}{\partial t}=0. \tag{1}$$

The terms of Eq. (1) represents respectively: flexural force, pressure and tension, centrifugal force, Coriolis force, inertia force, structural damping force and viscous damping force. Ω is the circular frequency of the tube.

He then explained how to transform this differential equation into a system of equations that can be solved. The solution process is simplified by the transformation of the variables into dimensionless form, via

$$\begin{aligned}&\xi=\frac{x}{L}, \quad \eta=\frac{y}{L}, \quad \tau=\left(\frac{EI}{M+m}\right)^{1/2}\frac{t}{L^2}, \quad \omega=\left(\frac{M+m}{EI}\right)^{1/2}\Omega L^2,\\ &u=\left(\frac{M}{EI}\right)^{1/2}UL, \quad \beta=\frac{M}{M+m}, \quad \gamma=\pm\frac{M+m}{EI}gL^3, \quad \kappa=\left(\frac{EI}{M+m}\right)^{1/2}\frac{k}{L},\end{aligned} \tag{2}$$

The system of equations is expressed as a summation of modes in Eq. (3), that is

$$\sum_{r=1}^{\infty}\{[(1+\mu i)\lambda_r^4+\kappa\omega i-\omega^2]\delta_{rj}+[u^2-\gamma]c_{rj}+\gamma d_{rj}+[\gamma+2\beta^{1/2}u\omega i]b_{rj}\}a_r=0,\ j=1,2,3\ldots, \tag{3}$$

b, c and d are coefficients defined and derived by Paidoussis (1998) and δ is the Kronecker function. The form of Eq. (3) is similar to the classical mode summation response equation expressed as

$$\eta(\xi,\tau)=\sum_{r=1}^{\infty}a_r\phi_r(\xi)e^{i\omega\tau} \tag{4}$$

Since all cylinder characteristics are known, the dimensionless flow velocity, u, and the dimensionless frequency, ω, are the only unknowns in Eq. (3). The sign of the imaginary part of the frequency term defines the stability of the response. To find the critical frequency of the tube at instability, the imaginary part of the frequency term is set to zero. Thus, the two unknowns are effectively real values. The solution of the system of equations is obtained by allowing the determinant of the coefficients of a_r to be equal to zero. This determinant has a real and an imaginary part. Equating each of those parts to zero yields a system of two equations and two unknowns, which can be solved.

2.2. Two-phase flow

To consider two-phase flow, the flow related terms in the above equations, in particular the mass, M, and the velocity, U, must be defined differently. To find appropriate formulation for those terms it is necessary to respect force equilibrium conditions. Considering that the different phases may have different flow velocities, it would be incorrect to use an averaged velocity to formulate both Coriolis and centrifugal forces. Thus, each of the phases is considered to

create its own Coriolis and centrifugal forces. It is assumed that the forces contributed by each phase may be added in the following equation of instability. The resulting modified fluidelastic instability equation to consider two-phase flow is expressed as follows:

$$EI\frac{\partial^4 y}{\partial x^4}+(\sum_k M_k+m)g\left((x-L)\frac{\partial^2 y}{\partial x^2}+\frac{\partial y}{\partial x}\right)+\sum_k M_k U_k^2\frac{\partial^2 y}{\partial x^2}$$
$$+2\sum_k M_k U_k\frac{\partial^2 y}{\partial t\partial x}+(\sum_k M_k+m)\frac{\partial^2 y}{\partial t^2}+EI\frac{\mu}{\Omega}\frac{\partial}{\partial t}\left(\frac{\partial^4 y}{\partial x^4}\right)+k\frac{\partial y}{\partial t}=0. \tag{5}$$

The subscript k represents each phase. For a two-phase flow, k takes the values 1 and 2. M_k and U_k are the masses and the velocities of each phase.

This new equation is also expressed in dimensionless form as Eq. (6) to facilitate the solution. The total mass of the flow is simply the addition of the masses of each phase. As a result, the definition of two dimensionless variables changes slightly as expressed in Eq. (7). Each phase has its own dimensionless velocity. Thus, each term is expressed as a function of the mass and velocity of each phase instead of the averaged flow characteristics. Each phase also has its own mass ratio; thus,

$$\sum_{r=1}^{\infty}\left\{\left[(1+\mu\mathrm{i})\lambda_r^4+\kappa\omega\mathrm{i}-\omega^2\right]\delta_{rj}+\left[\sum u_k^2-\gamma\right]c_{rj}\right.$$
$$\left.+\gamma d_{rj}+\left[\gamma+2\sum\beta_k^{1/2}u_k\omega i\right]b_{rj}\right\}a_r=0. \tag{6}$$

$$u_k=\left(\frac{M_k}{EI}\right)^{1/2}U_k L,\quad \beta_k=\frac{M_k}{\sum_k M_k+m}. \tag{7}$$

The possibility of solving this equation is apparently compromised. Considering a two-phase flow, three unknowns appear in this equation while only the same two equations are available. The unknowns are the dimensionless velocity of each phase and the dimensionless frequency. The number of unknowns can be reduced to two by including a relationship between the two-phase velocities. The two-phase flow theory will provide this relationship.

3. Two-phase flow theory in vertical tubes

3.1. Definitions and flow patterns

It is not the intention here to provide a comprehensive review of the two-phase flow theory. Only the essential elements needed in the fluidelastic instability formulation will be presented. Three fundamental definitions are needed for this purpose: void fraction, volumetric quality and slip ratio (Collier and Thome, 1994; Lahey and Moody, 1993; Chisholm, 1983; Hewitt, 1978; Wallis, 1969).

The void fraction, α, is the ratio between the volume occupied by the gas, V_g, and the total volume, V, of the flow. Because the element of length, δx, is constant, the void fraction is also the ratio of the area occupied by the gas, A_g, over the total flow area, A_g+A_l:

$$\alpha=\frac{V_g}{V}=\frac{V_g}{V_g+V_l}=\frac{A_g\delta x}{A_g\delta x+A_l\delta x}=\frac{A_g}{A_g+A_l}. \tag{8}$$

The volumetric quality, ε_g, is the ratio of the gas volumetric flow rate, Q_g, over the total volumetric flow rate; i.e.,

$$\varepsilon_g=\frac{Q_g}{Q_g+Q_l}. \tag{9}$$

The slip ratio, K, is the velocity ratio between, the gas and the liquid phase,

$$K=\frac{U_g}{U_l}. \tag{10}$$

These three quantities are linked by the following expression:

$$\frac{1-\varepsilon_g}{\varepsilon_g}=\left(\frac{1-\alpha}{\alpha}\right)\frac{1}{K}. \tag{11}$$

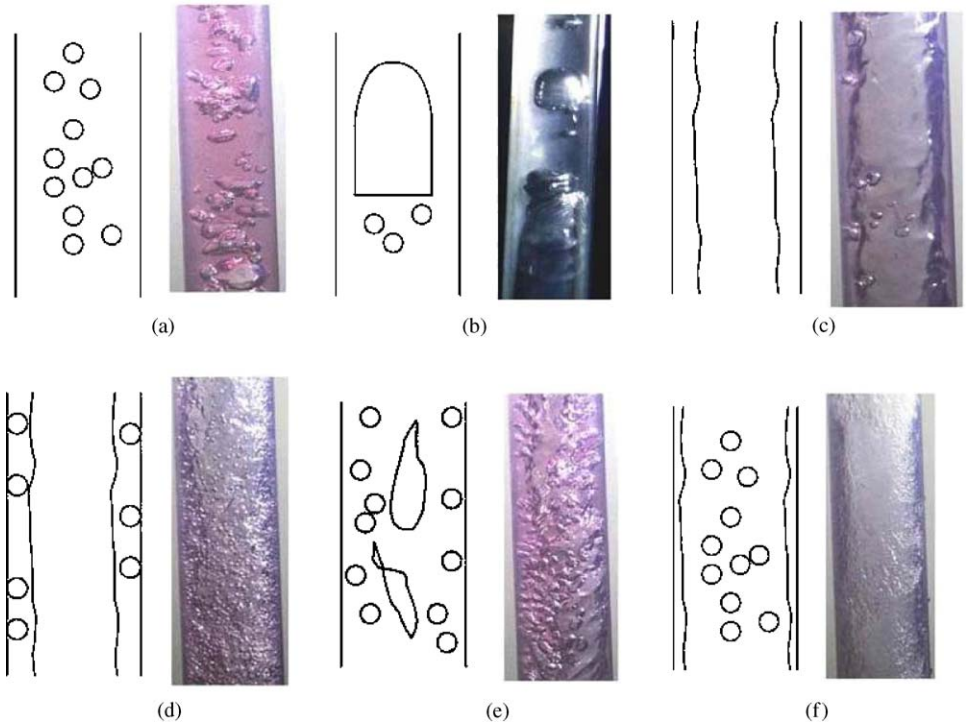

Fig. 1. Downward two-phase flow patterns:(a) bubbly flow, (b) slug (or plug) flow, (c) annular flow, (d) bubbly annular flow, (e) churn flow and (f) dispersed annular flow.

Different flow patterns or regime are possible in two-phase flow, depending on void fraction, flow rate, flow direction and flow path geometry. For downward flow, six possible flow patterns are described in the literature. All those flow patterns were observed in the laboratory, and photographs were taken. A comparison between those photographs and classical descriptions is presented in Fig. 1 for the different flow patterns.

3.2. Two-phase flow models

The homogenous model is the simplest two-phase flow model. This model proposes a slip ratio equal to one. Then, void fraction becomes equivalent to volumetric quality. With this model, the fluidelastic instability equation can be described with only one phase with average mass, M, and velocity, U. The average density may be calculated as follows:

$$\rho_H = \varepsilon_g \rho_g + (1 - \varepsilon_g)\rho_l. \tag{12}$$

Considering equal velocities for the two phases is probably not realistic. Chisholm proposes a model that describes the slip ratio as a function of volumetric quality and fluid properties (Chisholm, 1983). For high void fractions, Chisholm proposes a maximum value for the slip ratio, K_C:

$$K_C = \left(\frac{\rho_l}{\rho_H}\right)^{1/2} = \frac{1}{[1 - \varepsilon_g(\rho_g/\rho_l)]^{1/2}} \tag{13}$$

with a maximum of $K_C = (\rho_l/\rho_g)^{1/4}$.

Chisholm demonstrated that this model is in very good agreement with experiments (Chisholm, 1983). However, this model was derived for upward flow where the slip ratio is always higher than one. This suggests a gas velocity always higher than the liquid velocity. Some observations of downward flow patterns indicate that the liquid might possibly have a higher velocity than the gas. This is particularly obvious for slug flow. The shape of the top of the bubble gives the impression that the bubble is going upward. But because it is going downward, the velocity of the liquid around the bubble is definitely higher than the velocity of the bubble itself. Thus, the slip ratio should be less than one for bubble or

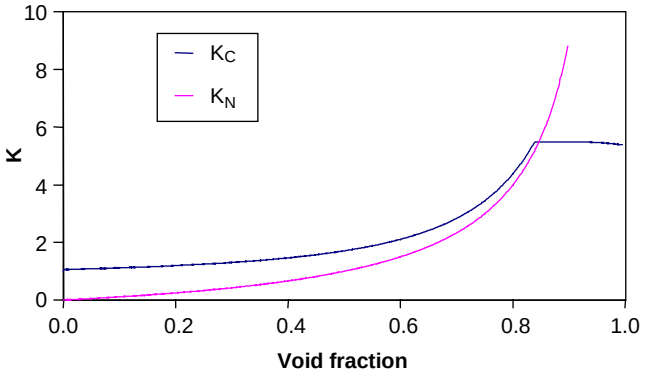

Fig. 2. The new (K_N) and Chisholm's (K_C) slip ratios for different void fractions.

slug downward flow. Because those two patterns are observed only at low void fraction, the slip ratio will be considered less than one for void fraction less than 50%. Chisholm gets relatively good agreement with experiments, even with downward flow and especially for high void fraction. It is thus reasonable to use a slip ratio close to Chisholm's ratio for void fraction higher than 50%. A simple expression to describe a new model for the slip ratio of downward flow is proposed in Eq. (14). This new slip ratio, K_N, is equivalent to the area ratio occupied by each of the phases:

$$K_N = \frac{A_g}{A_l} = \frac{\alpha}{1-\alpha} = \left(\frac{\varepsilon_g}{1-\varepsilon_g}\right)^{1/2}. \tag{14}$$

Also, K_N appears consistent with the observed flow patterns and is not very different from Chisholm's slip ratio as shown in Fig. 2.

4. Experiments

4.1. Test-section

The choice of tubes for the test-section was critical. Flexibility was the first criterion. Tubes had to be flexible enough to allow a visual observation of the fluidelastic instability phenomenon at reasonably low flow velocities. Because flow patterns had to be observed, transparency was a second criterion for the test-section. Diameters, lengths and linear masses of different test tubes had to be varied enough to provide validity of the results over a reasonable range of parameters. Flexible plastic tubes of Tygon R-3606 were chosen. A special procedure was developed to make sure the tubes were nominally straight. Table 1 outlines the characteristics of the different tubes used in the experiments.

4.2. Flow loop

In the experiments, two-phase flows were simulated with air–water mixtures. Although industrial piping systems are often subjected to vapour–liquid flows such as steam–water, air–water was used here because it is simple and reasonably realistic. It allows operating at ambient temperature and pressure. Water from two small pumps and service air were brought together and homogenised in a fine mesh air–water mixer. The pressure was controlled with a pressure regulator working in the range of 0–207 kPa. Pressure and volumetric flow rates were measured before the mixer. The pressure of the two-phase flow was also taken just before the test-section. Water returned to the tank after flowing out of the tube. The important parts of this experimental assembly are shown in Fig. 3.

4.3. Test procedure

The volumetric flow rates for each of the phases and the critical frequency were measured at the threshold of instability. An appropriate way to take flow rate measurements in single-phase flow is described by Paidoussis, (1970). A similar method was used to initiate the instability in two-phase flow and to take the measurements. The volumetric

Table 1
Test-section characteristics

	Inside diameter (mm)	Linear mass (g/m)	Length (m)
Tube A	6.35	47.4	0.7580
Tube B	9.25	65.7	0.3305
			0.3365
			0.5470
			0.8230
			1.1680
Tube C	12.7	87.8	0.3985
			0.5940
			0.6930
			0.7580
			0.9985
			1.1225
Tube D	12.7	186.0	0.2960
			0.4110
			0.5600
Tube E	12.7	618.0	0.9670
			1.5990
			1.4020

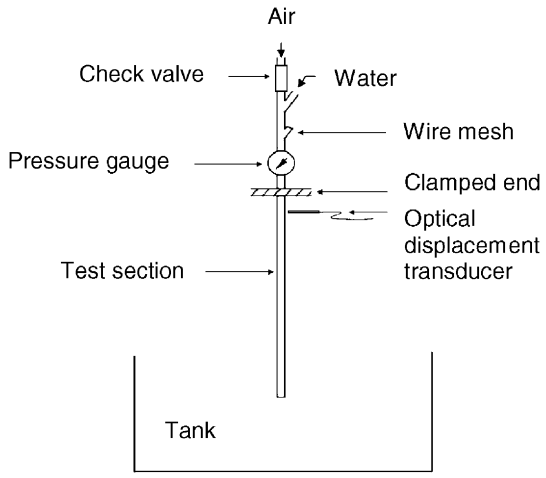

Fig. 3. Experimental assembly.

flow rate of water was set to a specific value. The volumetric flow rate of the air was gradually increased. Between each increase of the air-flow rate, enough time was allowed for the instability to develop. When the instability is reached, volumetric flow rate of air and water were measured. The volumetric flow rate of air was calculated with reference to the pressure in the test-section. The instability frequency was measured with an optical displacement sensor placed near the clamped end of the cantilevered tube.

5. Results

5.1. Damping coefficients and rigidity

The tube characteristics, which were needed to solve the fluidelastic instability equation (Eq. (6)), were the damping coefficients, μ and κ, and the flexural rigidity, EI. They were deduced from the measured frequency, $\mathrm{Re}(\Omega_1)$, and

logarithmic decrement, δ_1, for the first mode of free vibration of the tubes by the method described by Paidoussis (1998). The dimensionless parameter γ is found from its relation with the quantity $g/[\mathrm{Re}(\Omega_1)^2 L]$. EI is calculated from γ. Damping coefficients are found from the following relations: $[\chi\, Re(\omega_1) + \mu]/\delta_1 = Re(\omega_1)^2/[\pi(\lambda_1)^4]$ and $\kappa = \chi(\lambda_1)^4$. The hypothesis of $\chi\, Re(\omega_1) = \mu$ is used for small $\mathrm{Im}(\omega_1)$. This is explained in details in Paidoussis (1998). Damping values of $\mu = 0.1$ and of $\kappa = 0.12$ were found to be representative for all the tubes. Flexural rigidities, EI, were different for each tube as shown in Table 2.

5.2. Single-phase flow results

Although not the main topic of this paper, tests were done in single-phase flow to demonstrate the validity of the experimental procedure and of the damping model. Tests in single-phase flow were done for different lengths of Tube C in both water and air. The experimental results are presented in Table 3 and are compared to the theory in Figs. 4 and 5. As can be observed, the agreement is remarkably good. The validity of the experimental procedure and of the damping model is thus demonstrated.

5.3. Two-phase flow results

Three different two-phase flow models were considered. These models were compared to find out, which gave the best fit to the fluidelastic instability theory. Tube B with a length of 0.547 m was chosen to make this comparison. The results are presented in Figs. 6 and 7. The homogenous model, as expected, is by far the worst. The agreement between the theory and the experimental results is much better for the Chisholm's model. However, the agreement for low void fractions can be improved. The best fit is found with the new model which has more physical basis for low void fraction. The experimental results for all the other tubes are compared to the theory only for the new model for conciseness and expediency. Figs. 8 and 9 present the comparisons between the theory and results for Tube C of length 0.758 m, D of lengths 0.411 and 0.56 m and E of lengths 0.967 and 1.402 m.

6. Discussion

In general, the agreement between the theory and the experimental results is very good. Many tube sizes have been used in the experiments to demonstrate the validity of the model over a wide range of parameters. The theory combined with the new two-phase flow model has been validated for different mass ratio β from 0 to 60% and for different values of γ from 30 to 160. However, the agreement for Tube E is not quite as good, especially for higher void fraction. As it was the heaviest tube used in the experiments, the critical flow rate to reach the instability was a lot higher. Thus, the application of the proposed model beyond the range of parameters studied here should be done with great care. In reality, two-phase flows are very complicated and can not be described by a single relation between the phase velocities. Increasing flow rate or increasing void fraction may change the flow pattern. Phase interactions may be quite different for different flow patterns. Phase velocity ratio may also change with an increase in flow rate. A better model would be one that would consider changes in phase velocity ratio not only with changes in void fraction, but also with changes in total volumetric flow rate. Another way to consider flow pattern influence would be to define $(MU)_{\mathrm{eq}}$ and $(MU^2)_{\mathrm{eq}}$ related to flow considerations. Even if in these experiments bubbly flow was observed most of the time, other flow patterns may have appeared and changed the way each phase interact with the tube.

It is known that two-phase flow often results in significant damping. However, no information or measurements of such damping due to internal two-phase flow was available. Although, in the relatively small diameters of the tubes tested, relative motion between the liquid and gas phases may be limited. Furthermore, the instability phenomenon may not be sensitive to damping as indicated in Figs. 4 and 5. In this study, two-phase damping was assumed negligible. However, further studies should consider this aspect.

Although instability modes were not directly measured, some visual observations should be discussed. Fluidelastic instability modes in single-phase flows have been well described by Paidoussis (1970,1998). The mode observed at instability is dependent on the mass ratio and the parameter γ. The same tube undergoes instability in the first mode in air and in the fourth mode in water. In two-phase flows, the mass ratio is varied between that of air and that of water. For the same tube, instabilities in the first to fourth mode can be observed in two-phase flows. Observation of the first, the third and the fourth modes is shown in Fig. 10. The instability modes are unstationary, which means that nodes are moving along the tube. This motion is the results of an infinite addition of normal modes, as described by the

Table 2
Flexural rigidities of test-sections

	EI (Nm^2)
Tube B	0.003
Tube C	0.007
Tube D	0.018
Tube E	0.129

Table 3
Experimental results in single-phase flow

L (m)	Water flow		Air flow	
	$\beta = 0.5907$		$\beta = 0.0018$	
	U_c (m/s)	F (Hz)	U_c (m/s)	F (Hz)
0.3985	7.05	5.23	70.61	2.67
0.5940	5.61	3.63	56.49	1.55
0.6930	5.55	3.56	52.03	1.33
0.7580	5.47	3.32	51.10	1.22
0.9985	5.50	3.30	49.42	1.02
1.1225	5.41	3.50	49.80	0.96

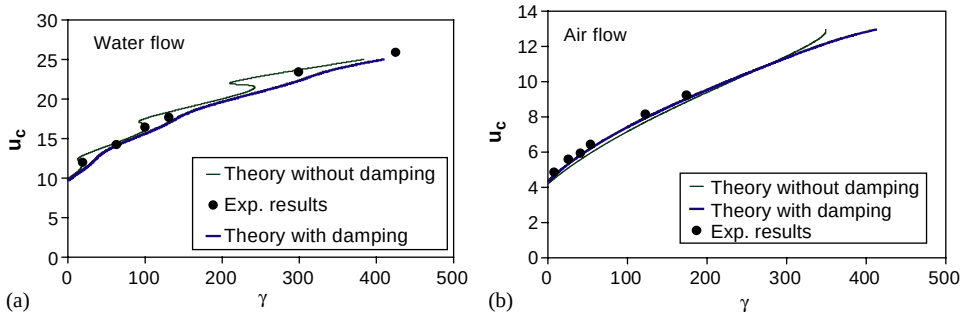

Fig. 4. Dimensionless critical velocity in single-phase flow for Tube C: (a) water flow and (b) air flow.

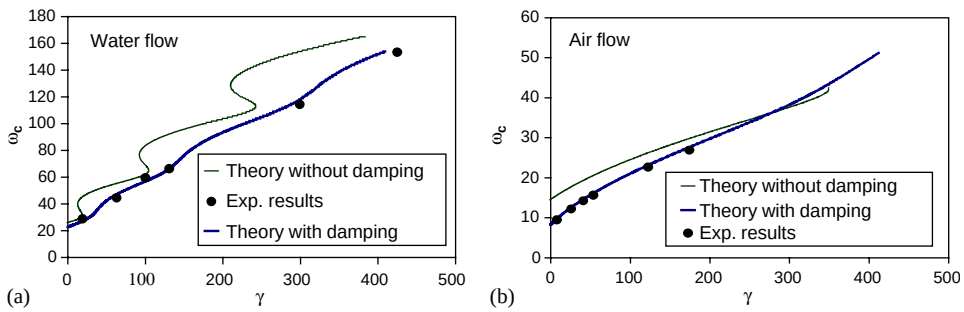

Fig. 5. Dimensionless critical frequency in single-phase flow for Tube C: (a) water flow and (b) air flow.

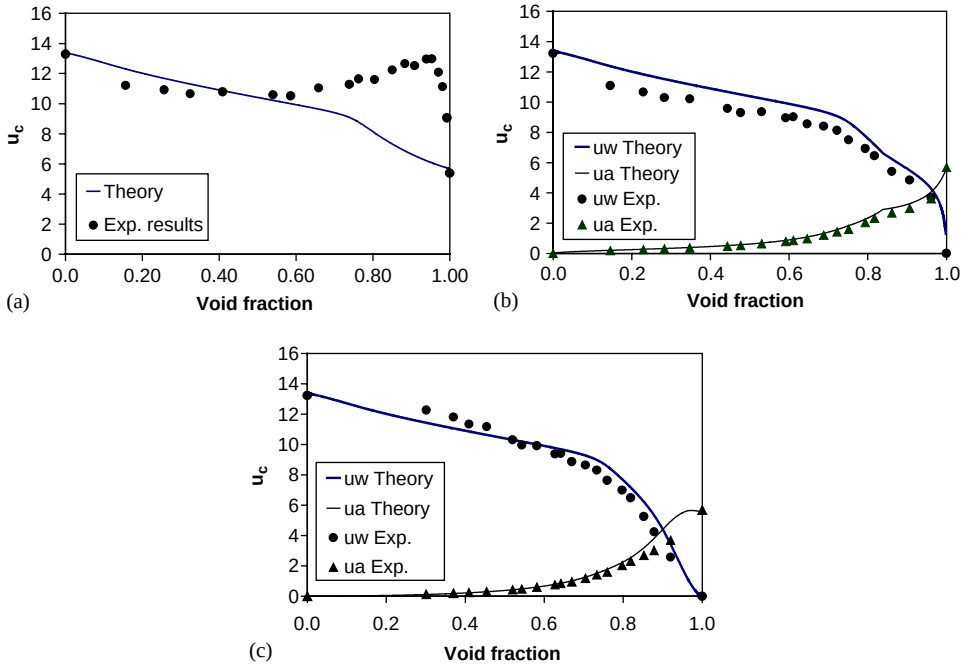

Fig. 6. Dimensionless critical velocity in two-phase flow for Tube B, $L = 0.547$ m: (a) homogeneous model; (b) Chisholm's model and (c) new model.

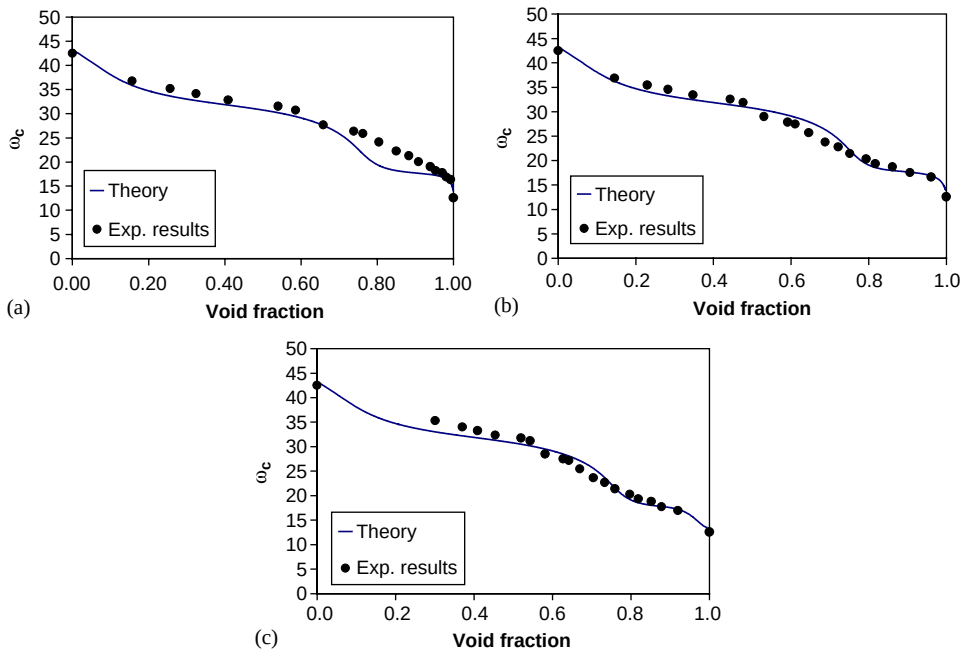

Fig. 7. Dimensionless critical frequency in two-phase flow for Tube B, $L = 0.547$ m: (a) homogeneous model; (b) Chisholm's model and (c) new model.

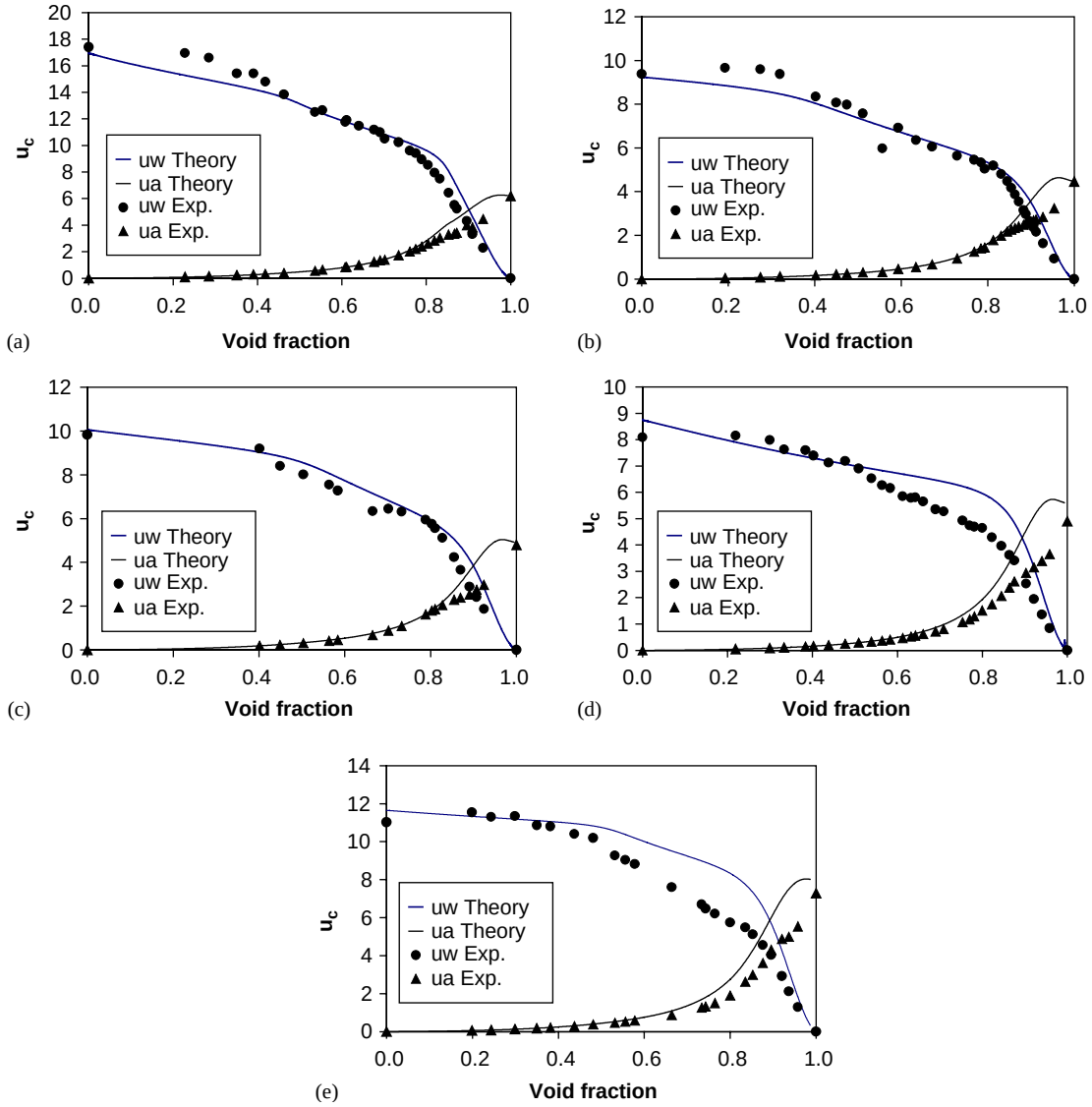

Fig. 8. Dimensionless critical velocity with new two-phase flow model: (a) Tube C, $L = 0.758$ m; (b) Tube D, $L = 0.411$ m; (c) Tube D, $L = 0.56$ m; (d) Tube E, $L = 0.967$ m and (e) Tube E, $L = 1.402$ m.

fluidelastic instability response formulation:

$$\eta(\xi,\tau) = \sum_{r=1}^{\infty} a_r \phi_r(\xi) e^{i\omega\tau}.$$

Two other observations are worthy of mention. First, turbulence is stronger in two-phase flow than in single-phase flow for the same flow rate. This difference in turbulence levels results in much larger vibrations in two-phase flows than in single-phase flow. Tube A because of its very light mass experienced very large vibration amplitude due to two-phase flow turbulence. Those vibrations made it difficult for the observer to identify the threshold of instability. The differences between theory and experimental results for Tube A were thus mostly due to observation errors rather than to an inappropriate model. Consequently, those results are not reported here.

The second observation is about pressure drop at instability. Instability of the cylinder increased the pressure loss in the test section. This was deduced from the observation of a cycle between instability and stability. Critical flow

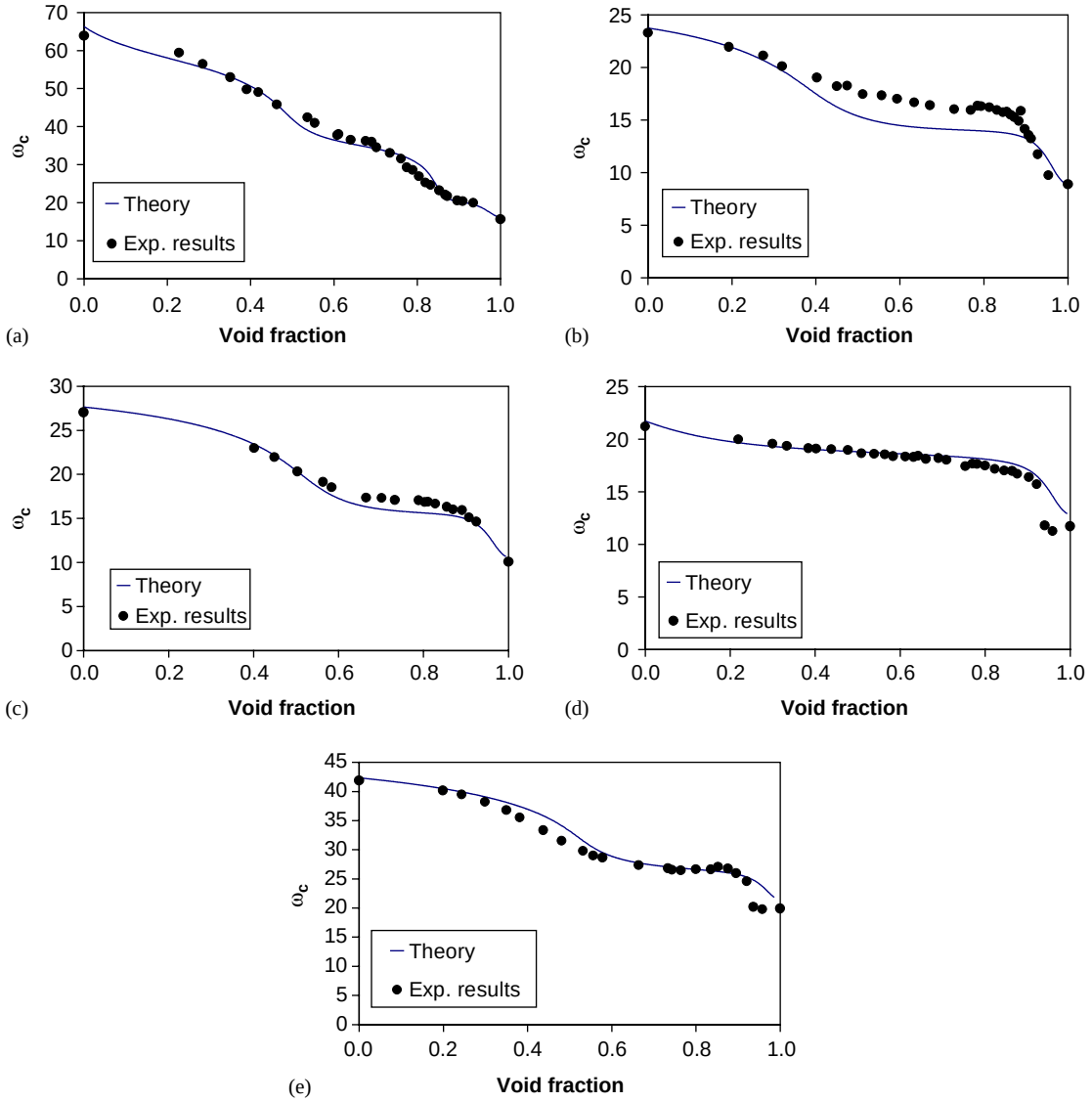

Fig. 9. Dimensionless critical frequency with new two-phase flow model: (a) Tube C, $L = 0.758$ m; (b) Tube D, $L = 0.411$ m; (c) Tube D, $L = 0.56$ m; (d) Tube E, $L = 0.967$ m and (e) Tube E, $L = 1.402$ m.

velocities were reached to initiate the instability. The instability increased the pressure drop, which reduced the water velocity below the critical velocity, which prevented instability. Water velocity was more affected than air velocity because water was provided to the loop by a small pump while air was provided by a relatively stable and constant pressure compressed air service. As the pressure loss decreased, the water velocity increased again beyond the critical velocity and instability resumed.

7. Conclusion

The fluidelastic instability behaviour of flexible tubes subjected to internal two-phase flows was investigated. Very well defined fluidelastic instabilities were observed over a broad range of parameters. The existing theory to formulate fluidelastic instability was extended to take into account two-phase flows. The agreement between the experimental

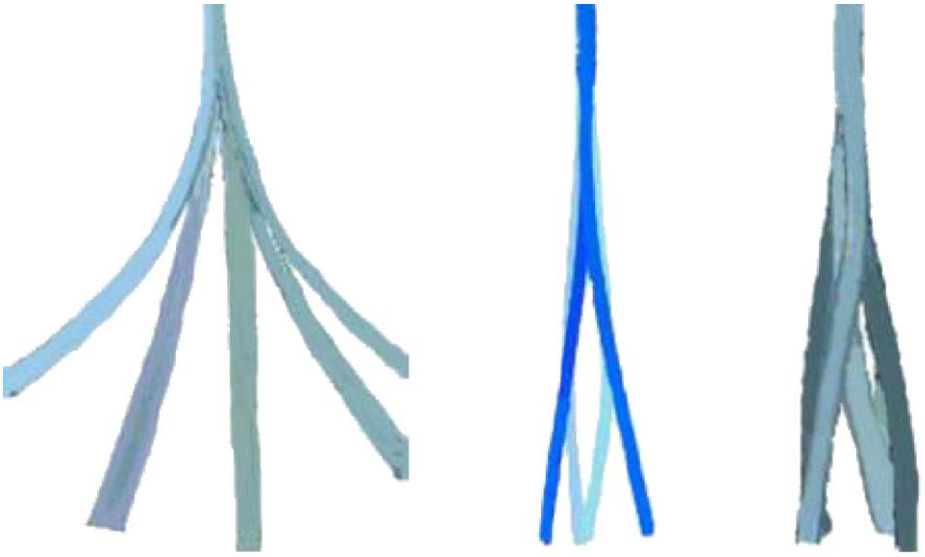

Fig. 10. Superposed digital photographs of fluidelastic instability modes: (a) 1st mode; (b) 3rd mode and (c) 4th mode.

results and the modified theory is remarkably good when an appropriate two-phase flow model is used to formulate the characteristics of two-phase flows. Such a model was developed based on the observed two-phase flow patterns during the experiments.

Acknowledgements

The authors are thankful to B. Besner and T. Lafrance who ably assisted with the construction of the experimental assembly and the measurements, and to L. Bulota who designed the two-phase mixer. The authors are grateful for the financial support of the Natural Sciences and Engineering Research council of Canada (NSERC) within the BWC/AECL/NSERC Industrial Research Chair in Fluid-Structure Interaction, and through an NSERC Discovery Grant. Also, the first author benefited from an NSERC Graduate Scholarship.

References

Axisa, F., Boheas, M.A., Villard, B., 1985. Vibration of tube bundles subjected to steam-water cross-flow: a comparative study of square and triangular arrays. Eighth International Conference on Structural Mechanics in Reactor Technology, Brussels, Belgium, August, Paper No. B 1/2.

Boucher, K.M., Taylor, C.E., 1996. Tube support effectiveness and wear damage assessment in the U-bend region of nuclear steam generators. Proceedings ASME Pressure Vessels and Piping Conference, Montréal, QC, Canada, July, PVP-vol. 328, Flow-Induced Vibration-1996, pp. 285–296.

Chisholm, D., 1983. Two-Phase Flow in Pipelines and Heat Exchangers. George Godwin, London, New York.

Collier, J.G., Thome, J.R., 1994. Convective Boiling and Condensation, third ed. Clarendon Press, Oxford.

Feenstra, P.A., Judd, R.L., Weaver, D.S., 1995. Fluidelastic instability of a tube array subjected to two-phase Rcross. Journal of Fluids and Structures 9, 747–771.

Feenstra, P.A., Weaver, D.S., Judd, R.L., 2002. Modelling two-phase flow-excited damping and fluidelastic instability in tube arrays. Journal of Fluids and Structures 16 (6), 811–840.

Hewitt, G.F., 1978. Measurement of Two-Phase Flow Parameters. Academic Press, London, New York.

Lahey Jr., R.T., Moody, F.J., 1993. The Thermal-Hydraulics of A Boiling Water Nuclear Reactor, Second ed. American Nuclear Society.

Nakamura, T., Fujita, K., Kawanishi, K., Yamaguchi, N., Tsuge, A., 1995. Study on the vibrational characteristics of a tube array caused by two-phase flow. Part II: Fluidelastic vibration. Journal of Fluids and Structures 9, 539–562.

Paidoussis, M.P., 1970. Dynamics of tubular cantilevers conveying fluid. IMechE Journal Mechanical Engineering Science 12 (2), 85–103.

Paidoussis, M.P., Pettigrew, M.J., 1979. Dynamics of flexible cylinders in axisymmetrically confined axial flow. ASME Journal of Applied Mechanics 46 (1), 37–44.

Paidoussis, M.P., 1998. Fluid–Structure Interactions: Slender Structures and Axial Flow. vol. 1, Academic Press, London.

Pettigrew, M.J., Paidoussis, M.P., 1975. Dynamics and stability of flexible cylinders subjected to liquid and two-phase axial flow in confined annuli. Paper D2/6, Proceedings of the Thrid International Conference on Structural Mechanics in Reactor Technology, London, UK, September 1–5.

Pettigrew, M.J., Taylor, C.E., 1994. Two-phase flow-induced vibration: an overview. ASME Journal of Pressure Vessel Technology 116 (3), 233–253.

Pettigrew, M.J., Tromp, J.H., Taylor, C.E., Kim, B.S., 1989. Vibration of tube bundles in two-phase cross-flow: Part 2, Fluidelastic instability. ASME Journal of Pressure Vessel Technology 111 (4), 478–487.

Pettigrew, M.J., Taylor, C.E., Jong, J.H., Currie, I.G., 1994. Vibration of a triangular tube bundle in two-phase freon-cross-flow. ASME Journal of Pressure Vessel Technology 117 (4), 321–329.

Pettigrew, M.J., Taylor, C.E., Janzen, V.P., Whan, T., 2002. Vibration behavior of rotated triangular tube bundles in two-phase cross-flows. ASME Journal of Pressure Vessel Technology 124 (2), 144–153.

Wallis, G.B., 1969. One-Dimensional Two-Phase Flow. McGraw-Hill Book Company, USA.